CMIR: a unified cross-modality framework for preoperative accurate prediction of microvascular invasion in hepatocellular carcinoma

之江实验室
ZHEJIANG LAB

liujinglj@zhejianglab.com

Jing Liu

Associate Researcher
Zhejiang Lab

Microvascular Invasion in HCC

- MVI is an independent risk factor for recurrence and survival after surgery or transplantation in HCC patients (5-year overall survival rate is 10%-20%).
- Postoperative histopathological diagnosis of MVI is difficult to meet the requirements of preoperative diagnosis.

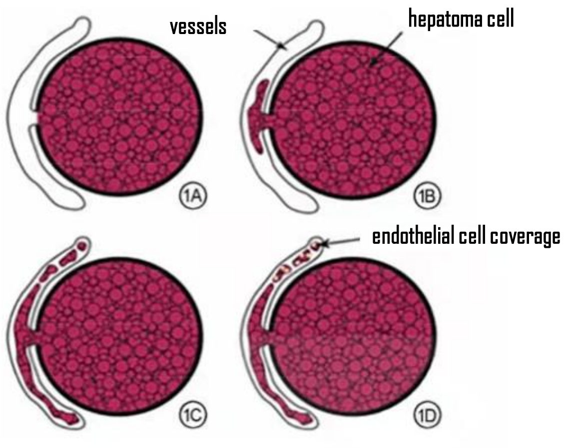

Fig 1. A schematic diagram of the microvascular invasion process in Hepatocellular Carcinoma Cell [1].

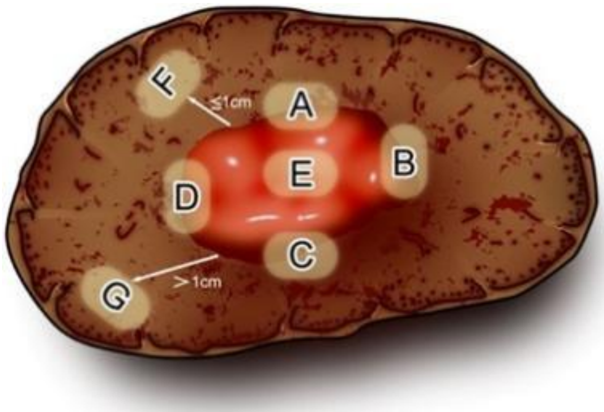

Fig 2. Schematic diagram of baseline sampling sites for liver tumor specimens[1].

1. M0: no MVI;
2. M1 (low-risk), MVI < 5 and at ≤ 1 cm away from the adjacent liver tissue;
3. M2 (high-risk), MVI > 5 or at > 1 cm away from the adjacent liver tissue.

[1] Wang, W., Guo, Y., Zhong, J. et al. The clinical significance of microvascular invasion in the surgical planning and postoperative sequential treatment in hepatocellular carcinoma. Sci Rep 11, 2415 (2021).

Radiomics Methods

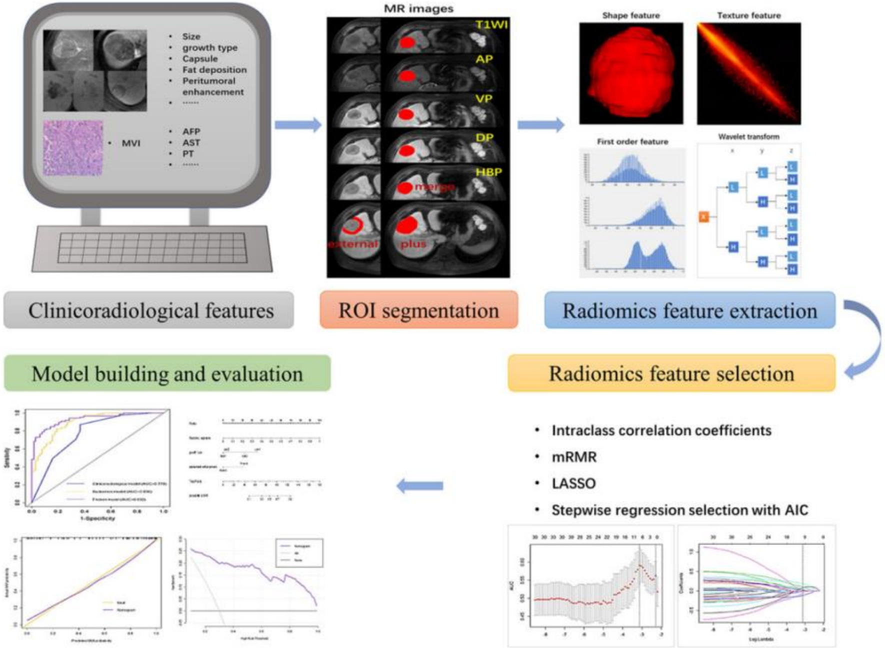

Fig 3. Flowchart of radiomics analysis for MVI prediction [2].

- Hand-crafted features
- Rely on human subjective judgment
- Low-level features

[2] Yang et al. Front. Oncol. 11:756216. doi: 10.3389/fonc.2021.756216

Radiomics Methods

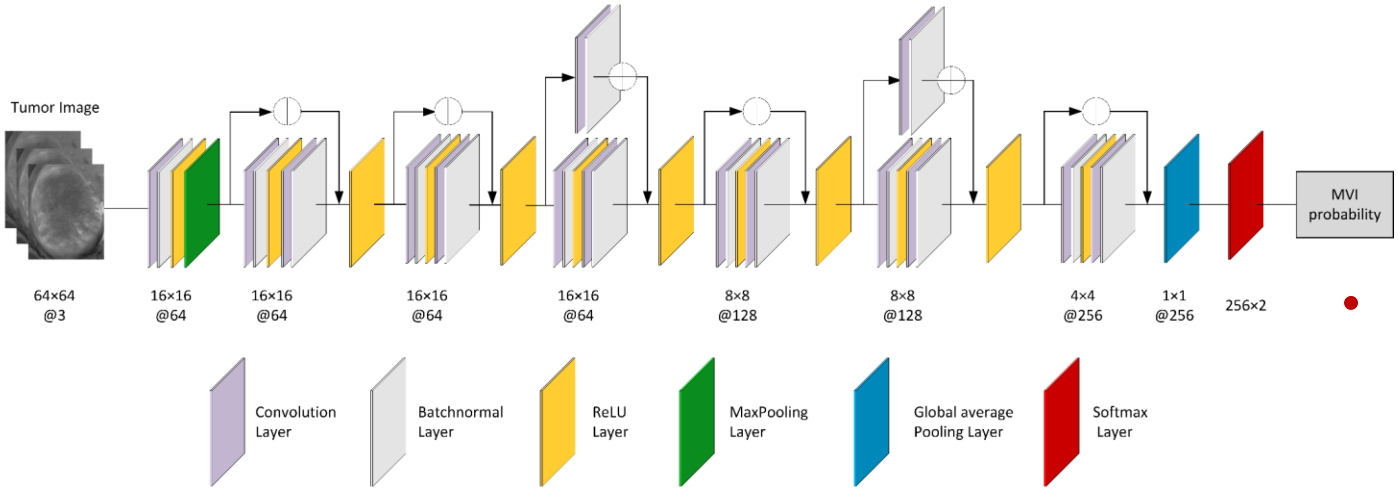

Fig 4. Deep learning models for MVI prediction [3].

- Single modality
- Low accuracy

- Poor interpretability
  (not suitable for clinical use)

[3] Wei et al. Cancers (Basel). 2021 May 14;13(10):2368.

Proposed Method

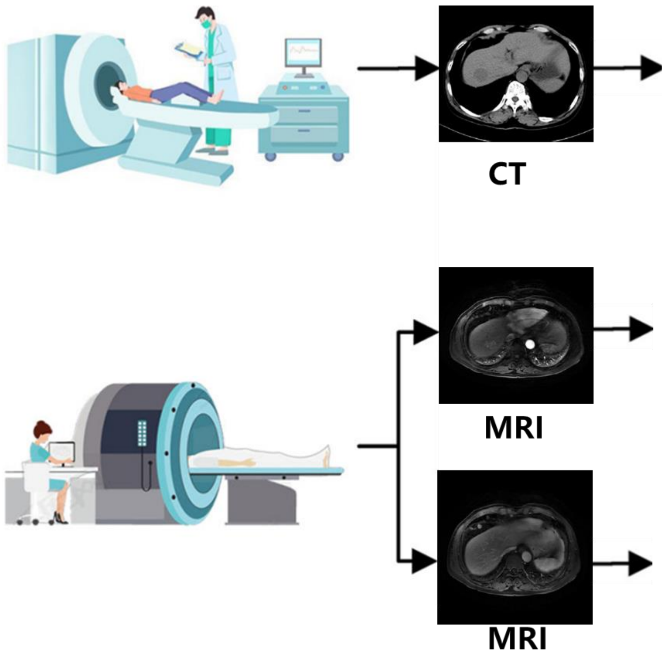

Able to distinguish tissues with density differences, but has limited resolution for soft tissues.

Has good resolution for soft tissues, but spatial resolution is lower than that of CT.

Presence of complementary information, joint prediction can improve prediction accuracy.

Proposed Method

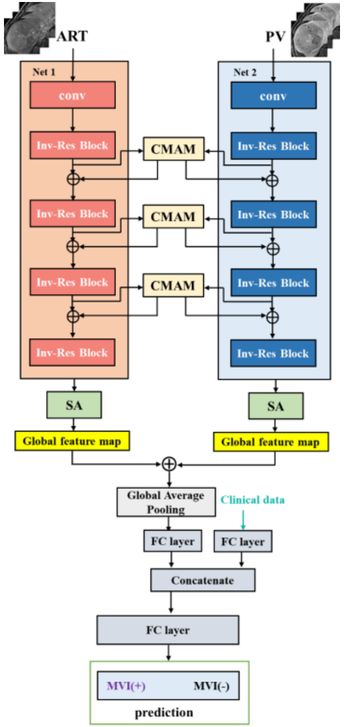

Fig 4. CMIR: a unified cross-modality framework.

$$Y_{i,j,k} = \sum_{(u,v)\in\Delta k} \mathcal{H}_{i,j,u+[K/2],v+[K/2],[KG/C]} X_{i+u,j+v,k},$$

$$\mathcal{H}_{i,j} = \phi(X_{i,j}) = W_1\sigma(W_0 X_{i,j}),$$

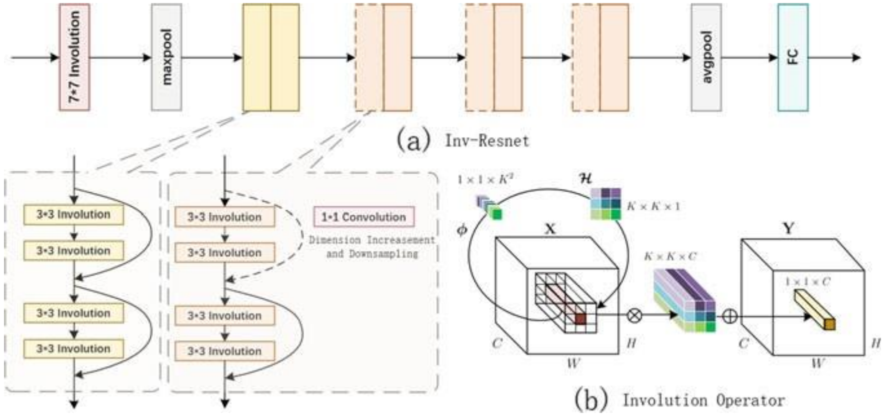

Fig 5. Inv-ResNet schematic diagram and involution operator. (a) Schematic diagram of Inv-ResNet. Two types of residual blocks are shown in the figure. In the convolution operation block, some convolution operations are replaced by Involution operations. (b) Abstract representation of Involution operator.

Proposed Method

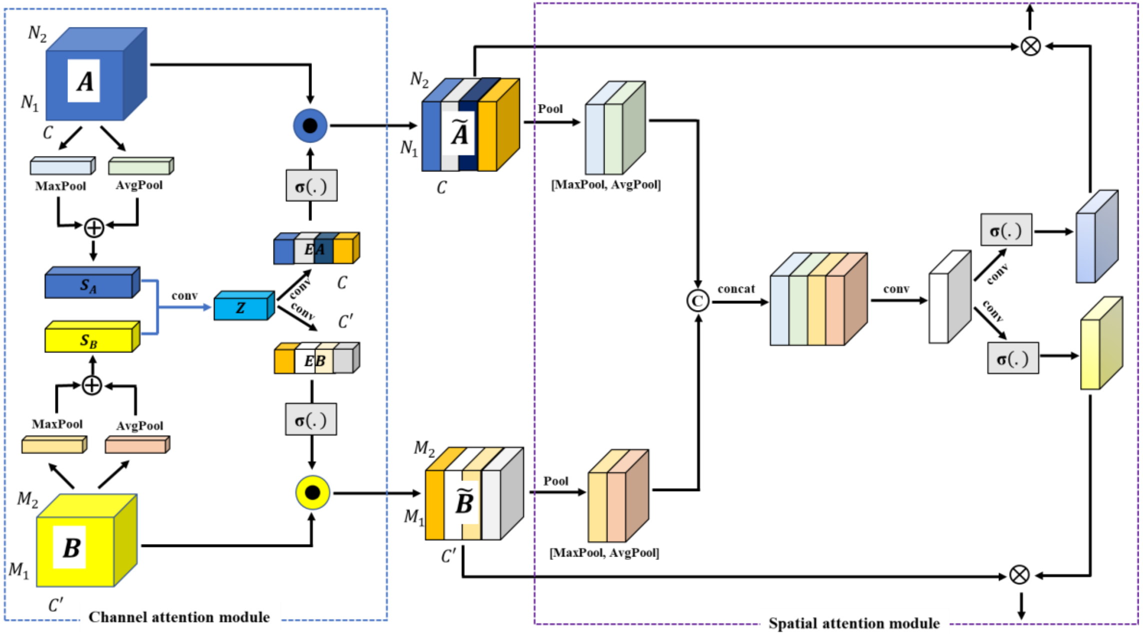

Fig 6. CMAM module.

Proposed Method

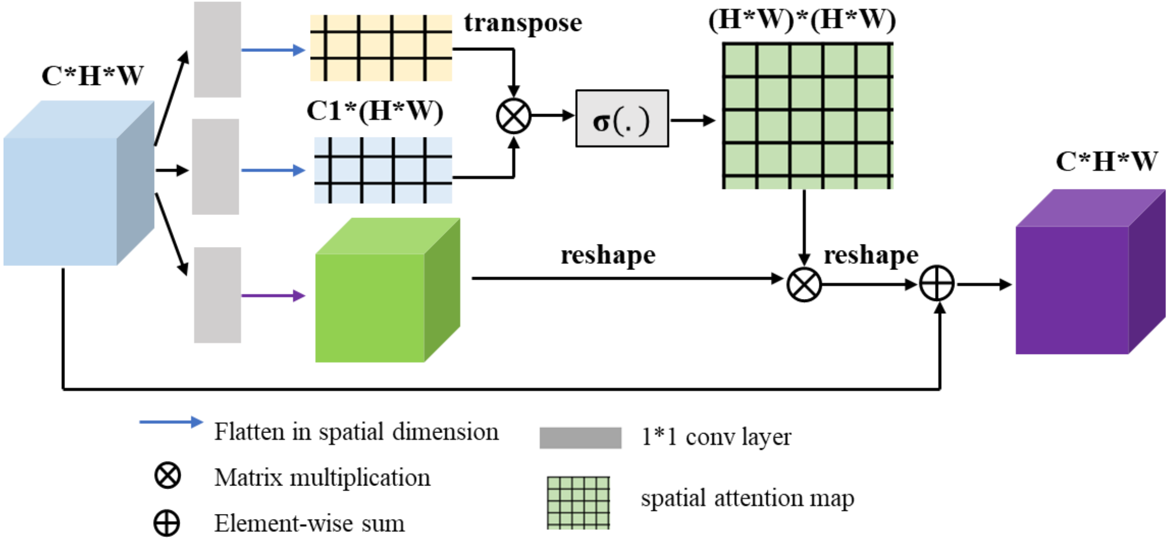

Fig 7. SA Localization Module.

Dataset

Table 1. Multi-phase MRI dataset.

	Training set	Internal validation set	External validation set			
Hospital name	Zhejiang Province Run Run Shaw Hospital (RRSH)	Zhejiang Province Run Run Shaw Hospital (RRSH)	The First Provincial Wenzhou Hospital of Zhejiang (FPWH)	Li Huili Hospital (LHH)	Zhejiang Taizhou Hospital (ZTH)	Zhejiang First Hospital (ZFH)
Number of cases	406		130	102	185	79
MVI (+)	124	31	42	61	40	20
MVI (-)	201	50	88	41	145	59
Positive and negative ratio	1:1.62	1:1.61	1:2.1	1:0.67	1:3.625	1:1.97

Preprocessing

Fig 8. Typical images of MVI preprocessing on ART and PV.

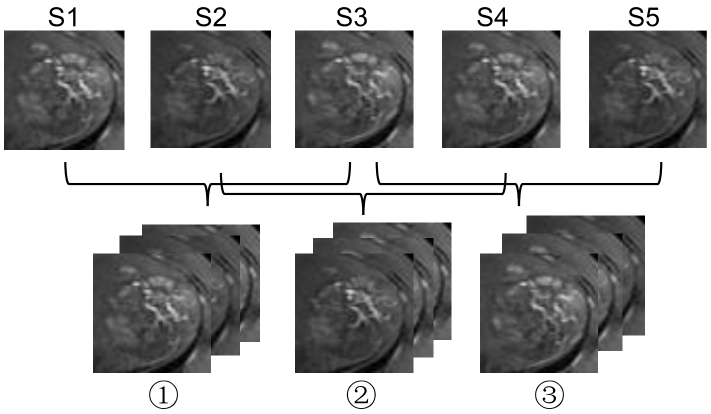

Fig 9. Combination of three-channel images.

Ablation Study

Table 2. The results of ablation study on different components.

Methods	Model Architecture					Evaluation Index			
	Single-phase	Multi-phase	Inv-block	CMAM	Multi-feature location module	ACC	AUC	SEN	SPE
S1	√					0.721	0.742	0.704	0.736
M1		√				0.776	0.784	0.785	0.753
M2		√	√			0.791	0.810	0.802	0.797
M3		√	√	√		0.839	0.842	0.865	0.801
Ours		√	√	√	√	**0.845**	**0.860**	**0.892**	**0.834**

Experiments and Results

Table 3. The results of the experimental comparison in five hospitals.

Method	Training set	Internal validation set	External validation set			
	RRSH	RRSH	FPWH	LHH	ZTH	ZFH
3D CNN-LSTM	0.874 (0.796, 0.803)	0.760 (0.740, 0.786)	0.702 (0.691, 0.711)	0.727 (0.700, 0.714)	0.673 (0.658, 0.696)	0.694 (0.684, 0.702)
DLC	0.880 (0.801, 0.798)	0.773 (0.752, 0.790)	0.700 (0.701, 0.706)	0.741 (0.724, 0.756)	0.713 (0.700, 0.708)	0.696 (0.692, 0.694)
IVIM	0.885 (0.812, 0.845)	0.782 (0.760, 0.798)	0.728 (0.720, 0.724)	0.755 (0.730, 0.759)	0.700 (0.708, 0.713)	0.721 (0.721, 0.752)
MVI-Mind	0.887 (0.824, 0.821)	0.789 (0.760, 0.800)	0.731 (0.734, 0.755)	0.756 (0.728, 0.764)	0.712 (0.723, 0.698)	0.720 (0.716, 0.768)
TED	0.903 (0.858, 0.819)	0.796 (0.787, 0.810)	0.735 (0.745, 0.769)	0.759 (0.741, 0.766)	0.715 (0.728, 0.717)	0.742 (0.754, 0.787)
Proposed	**0.926 (0.892, 0.834)**	**0.845 (0.814, 0.803)**	**0.794 (0.791, 0.786)**	**0.819 (0.806, 0.812)**	**0.767 (0.782, 0.778)**	**0.801 (0.816, 0.800)**

Conclusion

- We proposed a robust, high-precision cross-modal unified framework named CMIR based on multi-phase MR images and clinical data, and applies it to the accurate prediction of microvascular invasion in HCC.
- Three important feature extraction, fusion and localization modules Inv-ResNet, CPAM and SA are proposed, they enrich the semantic information across modalities and achieve the state-of-the-art performance on different hospitals.
- In future work, we plan to fuse more modalities such as genetic information and apply the proposed algorithm to clinical diagnosis.

Thank you for your attention